ELEMENTARY PARTICLES AND FIELDS
Theory

Method for Simulating Electroweak Top-Quark Production Events in the NLO Approximation: SingleTop Event Generator

E. E. Boos, V. E. Bunichev, L. V. Dudko, V. I. Savrin, and V. V. Sherstnev

Institute of Nuclear Physics, Moscow State University, 119992 Russia

Received September 2, 2005; in final form, December 29, 2005

Abstract—A new method for simulating electroweak top-quark production processes is described along with its computer realization in the SingleTop event generator. Special attention is paid to the correct combination of events from two parts of the main t-channel production process: $2 \to 2$ with a b quark in the initial state and $2 \to 3$, where an additional b quark appears in the final state. Integration of these two contributions enables the generation of event samples including the first correction to the leading perturbation order, avoiding the double-counting problem and negative-weight events. The SingleTop generator is based on the complete set of the tree Feynman diagrams calculated by the CompHEP package.

1. INTRODUCTION

After the discovery of the top quark at the Tevatron Collider [1] and measurement of its mass [2], the main problem of top quark physics is the detailed study of its properties within and beyond the Standard Model (SM). Owing to the large mass of the top quark, deviations from the SM predictions might be most likely observed in top-quark physics.

The top quark was discovered in the pair production process described by Feynman diagrams with the t and $\bar{t}$ quarks produced in the gluon interaction vertex. The single top-quark production is a production channel associated with the electroweak interaction of the top quark with the W boson and b quark. As mentioned by a number of authors [3], single top-quark production processes might provide precise information on the top-quark interaction vertices, in particular, on the structure of the Wtb vertex, which is responsible for the main decay channel of the top quark in the SM (the partial decay width is $\approx 99\%$) and is proportional to the matrix element V_{tb} of the Cabibbo−Kobayashi−Maskawa mixing matrix. The processes under consideration are highly sensitive because the top quark is produced in the Wtb vertex in contrast to the pair production.

The total cross section for single top-quark production (it reaches ≈ 300 pb at the LHC and ≈ 2.8 pb at the Tevatron) [4] is comparable in order of magnitude to the cross section for QCD pair production (≈ 800 pb at the LHC and ≈ 8 pb at the Tevatron) [4]. Owing to the relatively large cross section for the single top-quark production, this process forms a significant background for many other interesting processes, for example, for Higgs boson production. Therefore, the maximum precise kinematic description of the single top-quark production is needed not only for studying the properties of the top quark itself, but also for solving some other problems in high-energy physics.

There are three main production processes of the single top quark at the hadron colliders. Figure 1 displays the Feynman diagrams for all processes in the leading perturbation order (hereafter, the LO approximation). Figures 2 and 3 show the typical Feynman diagrams for the t- and s-channel processes in the next-to-leading perturbation order (the NLO approximation).

The single top-quark production at the hadron colliders was previously investigated in [3]. The authors of [5, 6] studied the most complete set of processes in the SM that contribute to the single top-
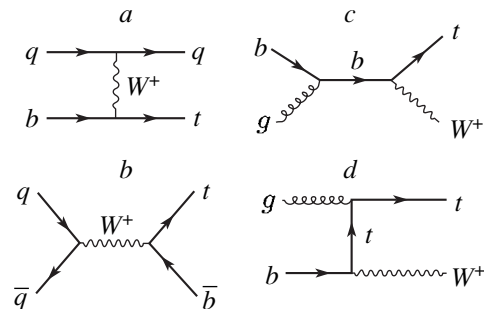
Fig. 1. Leading-order Feynman diagrams for the single top-quark production.
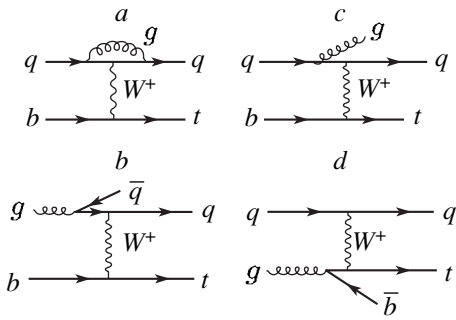
Fig. 2. Typical next-to-leading-order Feynman diagrams for the single top-quark production in the t-channel process.
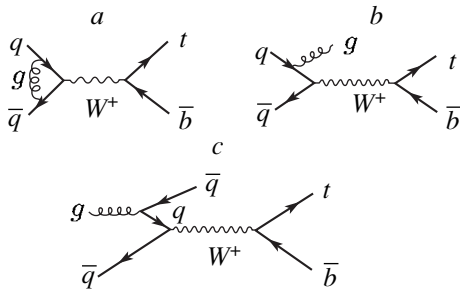
Fig. 3. Same as in Fig. 2, but for the s-channel process.

quark production; the authors of [4, 7–11] calculated the cross sections in the NLO approximation for the s- and t-channel processes. The complete Monte Carlo analysis of the production processes of the single top quark allowing for the main background effects was performed in [6, 12].

The processes of the single top-quark production were simulated using various packages, event generators (hereafter, simply events), based on Monte Carlo calculations (MC generators): ONETOP [13], TopReX [14], MC generators using the calculation packages MadGraph [8, 15] and CompHEP [6, 16], and PYTHIA MC generator [17]. However, none of these codes solves all problems associated with the correct and precise simulatioon of the single top-quark production processes; some of these problems are listed below.

(1) The combination of events corresponding to the diagram in Fig. 2a allowing for the parton showers in the initial state (ISR) and to the diagrams in Figs. 2b, 2c, and 2d results in double counting in part of the soft region with respect to P_T of the initial b quark, because the distribution of the b quark in the proton (hereafter, PDF) is determined from the kernel of the process $g \to b\bar{b}$ used also in the tree diagram in Fig. 2d. The direct application of the subtraction procedure in the t-channel process results in a negative weight for part of the events. We can improve the situation by subtracting the first term of the gluon splitting function $g^* \to b\bar{b}$ from the PDF of b quarks and, following [6], applying the modified function in all further calculations. This approach is free from negative-weight events, but the procedure faces problems in simulating the ISR in the PYTHIA generator owing to the nonstandard ISR. However, the ISR mechanism makes it possible to apply another method that gives the correct differential cross sections and simulates events for the t-channel process in the NLO approximation.

(2) As emphasized in [18, 19], the top quark is produced in electroweak processes with significant polarization owing to the $(V - A)$ structure of the Wtb vertex in the SM. As a result, spin correlations between the production and the decay of the top quark appear. Therefore, the correct MC generator should include these correlations.

(3) As we showed in [20], the single top-quark production processes are sensitive to the anomalous contributions to the Wtb vertex. In order to study many scenarios of extending the SM, the MC generator should include the corresponding anomalous operators in the Wtb vertex. In addition, it is necessary to include other anomalous vertices, for example, the neutral currents that change the quark flavor (FCNC), etc.

(4) At the LHC collider, t and $\bar{t}$ quarks are produced with different cross sections. The corresponding asymmetry in the kinematic distributions is useful for reducing the systematic errors in the measurement of the top quark parameters [20]. Therefore, it is necessary to have the possibility to separate the production models for t and $\bar{t}$ quarks at the level of the MC generator.

In this paper, we present the developed method of the effective NLO approximation for simulating the electroweak top-quark production processes that solves the listed problems and generates events including the NLO corrections. The method is realized using the SingleTop MC generator and widely used in the investigations performed by the collaborations D0 (Tevatron Collider at FNAL) and CMS (LHC Collider under construction at CERN). The method was first applied by the CMS Collaboration and described in [21]. In Section 2, we present the total cross sections for the single top-quark production in the LO and NLO approximations and describe the components required for the creation of the SingleTop MC generator. Section 3 describes the method of event generation in the effective NLO approximation for the t-channel process. In Section 4, we compare the effective NLO approximation with the calculations in the exact NLO approximation. Section 5 is devoted to the spin-correlation effects in the single

top-quark production processes. Section 6 contains conclusions.

2. CROSS SECTIONS FOR THE SINGLE TOP-QUARK PRODUCTION PROCESSES

It is convenient to classify the single top-quark production processes with respect to the virtuality of the W-boson Q_W^2 (the four-momentum squared of the W boson) that is involved in top-quark production.

The t-channel process ($Q_W^2 < 0$) has the maximum cross section at both the Tevatron and the LHC colliders. Subprocesses with the b quark in the initial state corresponding to the diagrams in Figs. 1a, 2a–2c will be called the $(2 \to 2)$ part of the process, and subprocesses corresponding to the diagram in Fig. 2d, where the b quark exists in the final state, will be called the $(2 \to 3)$ part of the process. The latter contribution is also known as Wg fusion.

The s-channel process ($Q_W^2 > 0$) in the leading perturbation order is described by one $2 \to 2$ diagram in Fig. 1b, where the top quark is produced together with the b quark from the virtual W boson. The cross section for this process in the SM at the energy of the Tevatron collider is lower than that of the t-channel process by a factor of 2.5; at the energy of the LHC collider, the cross section for the t-channel process exceeds that for the s-channel process by a factor of 25. However, the s-channel process is sensitive to the various possible deviations from the SM predictions.

The tW process, where the single top quark is produced together with the real W boson in the final state, corresponds to $Q_W^2 = m_W^2$. The cross section for the process is negligibly small at the Tevatron collider owing to the production of two massive particles in the final state. However, the process cross section is significant at the energy of the LHC collider. Since this process involves also the b quark in the initial state, there is the problem of combination of the contributions from the diagrams $2 \to 2$ and $2 \to 3$ (where the initial state contains the graph $g \to b\bar{b}$).

The first version of the SingleTop MC generator involves events for the s- and t-channel processes. The tW process gives a large contribution to the total cross section for the single top-quark production at the LHC, but has, in contrast to other processes, a significantly different signature of the final state similar to the pair top-quark production (which produces additional problems in the event generation [22]). The tW process is not included in the described version of the MC generator. We are going to add it in the next version of the SingleTop MC generator. In our calculations, we used the following values of the physical parameters:

masses and decay widths: $m_t = 175.0$ GeV, $\Gamma_t = 1.547$ GeV, $m_b = 4.85$ GeV, $m_c = 1.65$ GeV, $m_s = 0.117$ GeV, $m_W = 79.958$ GeV, and $\Gamma_W = 2.028$ GeV;

$\alpha = 1/127.9$, $\sin\theta_W = 0.480\,76$, $\alpha_s(m_Z) = 0.117$ (the PDF set determines the values and the evolution equation);

parton distribution functions cteq6m determined by the CTEQ group [23];

the value of the QCD factorization parameter chosen according to the condition of maximum closeness of the LO cross section to the NLO cross section [12], the resulting typical factorization scale being $Q_{QCD} \approx m_t/2$ and m_t for the t- for the s-channel processes, respectively [20].

Sullivan [9] showed that the NLO results for the s-channel process completely coincide with the LO calculations with a certain K factor. Therefore, the sample generation procedure for the s channel is very simple: we prepared the event samples for the $pp \to t\bar{b}$ and $pp \to \bar{t}b$ processes (for the Tevatron, the initial state is $p\bar{p}$) in the LO approximation, but used the NLO parton distribution functions cteq6m; then, we normalized the result to the NLO total cross section. Tables 1–4 present the LO and NLO cross sections. The resulting ratio of the cross sections is 1.3 for the LHC and 1.5 for the Tevatron.

Correct and precise simulation of the t-channel single top-quark production requires the inclusion of the significant contribution of the actual NLO correction with the gluon splitting $g \to b\bar{b}$ (the diagram in Fig. 2d). One of the methods for accurately including this correction is the combination of the $2 \to 2$ diagrams (with the b quark in the initial state) with the $2 \to 3$ diagrams (with the explicit inclusion of the $g \to b\bar{b}$ subgraph). In such combination, it is necessary to subtract the first term in the expansion of the gluon splitting function ($g \to b\bar{b}$) in order to avoid double counting in the parton distribution function and in the matrix element [3, 5, 12]. However, owing to the problems considered in the preceding section, we developed another simulation method for this correction, the method of the effective NLO approximation described in the next section. The method requires three components: events for the $pp \to tq(\bar{t}q)$ and $pp \to tq(\bar{t}q) + b$ processes and the NLO total cross section for the $pp \to tq + \bar{t}q$ process (for the Tevatron, the initial state is $p\bar{p}$). Table 3 contains the LO total cross sections for the t-channel t- and $\bar{t}$-quark production.

It is worth noting that the $pp \to tbg$ process has the same final state that the t-channel process has. However, it is natural to consider it as an NLO correction to the s-channel process and to take it into

Table 1. Leading-order total cross section (in pb) for the s-channel top-quark production obtained with the NLO parton distribution functions. The cross section for the $pp \to t\bar{b}(\bar{t}b)$ process is 4.96(3.09) pb at the LHC and the cross sections for the $p\bar{p} \to t\bar{b}$ and $p\bar{p} \to \bar{t}b$ processes at the Tevatron energy are both equal to 0.30 pb (numbers in parentheses)

Subprocesses							
$u\bar{d} \to t\bar{b}$	$\bar{d}u \to t\bar{b}$	$\bar{d}c \to t\bar{b}$	$c\bar{d} \to t\bar{b}$	$d\bar{u} \to \bar{t}b$	$\bar{u}d \to \bar{t}b$	$\bar{c}d \to \bar{t}b$	$s\bar{c} \to \bar{t}b$
$u\bar{s} \to t\bar{b}$	$\bar{s}u \to t\bar{b}$	$\bar{s}c \to t\bar{b}$	$c\bar{s} \to t\bar{b}$	$s\bar{u} \to \bar{t}b$	$\bar{u}s \to \bar{t}b$	$d\bar{c} \to \bar{t}b$	$\bar{c}s \to \bar{t}b$
2.22 (0.291)	2.22 (0.006)	0.26 (0.001)	0.26 (0.001)	1.285 (0.291)	1.285 (0.006)	0.26 (0.001)	0.26 (0.001)

Table 2. Next-to-leading order total cross section (in pb) for single top-quark production at $m_t = 175$ GeV [4]. The parton distribution functions cteq5m1 are used. The QCD scale is M_{tb} for the s-channel process. This scale is $\sqrt{-(\mathbf{p}_t - \mathbf{p}_b)^2}$ for the light-quark line and $\sqrt{-(\mathbf{p}_t - \mathbf{p}_b)^2 + m_t^2}$ for the heavy- quark line in the t-channel process. The error includes the statistical error 0.1−0.4% and the error from the variation of the QCD scale: ±5% for the Tevatron and ±2% for the LHC

Collider	Process	t	$\bar{t}$	$t + \bar{t}$
LHC	t channel	152.6 ± 3.1	90.0 ± 1.9	242.6 ± 3.6
	s channel	6.55 ± 0.14	4.1 ± 0.1	10.6 ± 0.17
Tevatron	t channel	0.95 ± 0.1	0.95 ± 0.1	1.9 ± 0.1
	s channel	0.44 ± 0.04	0.44 ± 0.04	0.88 ± 0.05

Table 3. Leading-order cross section (in pb) for the t-channel process with the cutoff $P_T(b) > 10$ GeV (the cutoff parameter choice is explained in Section 3) and with the NLO parton distribution functions. The cross sections for the $pp \to tq\bar{b}$ and $pp \to \bar{t}qb$ processes at the LHC energy are 82.3 and 47.9 pb, respectively. The cross sections for the $p\bar{p} \to tq\bar{b}$ and $p\bar{p} \to \bar{t}qb$ processes at the Tevatron energy are both equal to 0.379 pb (numbers in parentheses).

Subprocesses					
$ug \to dt\bar{b}$	$ug \to st\bar{b}$	$\bar{d}g \to \bar{c}t\bar{b}$	$\bar{u}g \to \bar{d}\bar{t}b$	$\bar{u}g \to \bar{s}\bar{t}b$	$dg \to c\bar{t}b$
$gu \to dt\bar{b}$	$gu \to st\bar{b}$	$g\bar{d} \to \bar{c}t\bar{b}$	$g\bar{u} \to \bar{d}\bar{t}b$	$g\bar{u} \to \bar{s}\bar{t}b$	$gd \to c\bar{t}b$
$cg \to dt\bar{b}$	$cg \to st\bar{b}$	$\bar{s}g \to \bar{c}t\bar{b}$	$\bar{c}g \to \bar{d}\bar{t}b$	$\bar{c}g \to \bar{s}\bar{t}b$	$sg \to c\bar{t}b$
$gc \to dt\bar{b}$	$gc \to st\bar{b}$	$g\bar{s} \to \bar{c}t\bar{b}$	$g\bar{c} \to \bar{d}\bar{t}b$	$g\bar{c} \to \bar{s}\bar{t}b$	$gs \to c\bar{t}b$
$\bar{d}g \to \bar{u}t\bar{b}$			$dg \to u\bar{t}b$		
$g\bar{d} \to \bar{u}t\bar{b}$			$gd \to u\bar{t}b$		
$\bar{s}g \to \bar{u}t\bar{b}$			$sg \to u\bar{t}b$		
$g\bar{s} \to \bar{u}t\bar{b}$			$gs \to u\bar{t}b$		
68.8 (0.328)	7.6 (0.03)	5.9 (0.021)	36.2 (0.328)	4.9 (0.03)	6.8 (0.021)

account when calculating the s-channel single top-quark production. Therefore, we omit the cross section for the $pp \to tbg$ process from the table of the LO cross sections for the t-channel process.

The developed event-generation procedure also requires the $pp \to tj(\bar{t}j)$ events, that is, the events in the LO approximation. Table 4 contains the cross sections for various subprocesses of this process. However, when combining such events with the events obtained for the $(2 \to 3)$ part, we will calculate the cross section based on the NLO total cross section (see the next section) rather than the numbers from Table 4. The NLO total cross sections for the s- and t-channel processes are taken from [4] and presented in Table 2 displays.

The SingleTop MC generator is based on the CompHEP package [16] designed for particle-physics calculations and the interface library

Table 4. Leading-order total cross section (in pb) for the t-channel top-quark production with the NLO parton distribution functions. The cross section for the $pp \to tj(\bar{t}j)$ process at the LHC energy is 155.39(89.85) pb. The cross sections for the $p\bar{p} \to t\bar{b}$ and $p\bar{p} \to \bar{t}b$ processes at the Tevatron energy are both equal to 0.966 pb (numbers in parentheses)

Subprocesses					
$ub \to dt$	$ub \to st$	$\bar{d}g \to \bar{c}t$	$\bar{u}\bar{b} \to \bar{d}\bar{t}$	$\bar{u}\bar{b} \to \bar{s}\bar{t}$	$d\bar{b} \to c\bar{t}$
$bu \to dt$	$bu \to st$	$g\bar{d} \to \bar{c}t$	$\bar{b}\bar{u} \to \bar{d}\bar{t}$	$\bar{b}\bar{u} \to \bar{s}\bar{t}$	$\bar{b}d \to c\bar{t}$
$cb \to dt$	$cb \to st$	$\bar{s}g \to \bar{c}t$	$\bar{c}\bar{b} \to \bar{d}\bar{t}$	$\bar{c}\bar{b} \to \bar{s}\bar{t}$	$s\bar{b} \to c\bar{t}$
$bc \to dt$	$bc \to st$	$g\bar{s} \to \bar{c}t$	$\bar{b}\bar{c} \to \bar{d}\bar{t}$	$\bar{b}\bar{c} \to \bar{s}\bar{t}$	$\bar{b}s \to c\bar{t}$
$\bar{d}b \to \bar{u}t$			$d\bar{b} \to u\bar{t}$		
$b\bar{d} \to \bar{u}t$			$\bar{b}d \to u\bar{t}$		
$\bar{s}b \to \bar{u}t$			$s\bar{b} \to u\bar{t}$		
$b\bar{s} \to \bar{u}t$			$\bar{b}s \to u\bar{t}$		
129.26 (0.869)	15.01 (0.057)	11.12 (0.040)	66.99 (0.869)	10.05 (0.057)	12.81 (0.040)

CPYTH [24] designed for the transition of the simulated events from the CompHEP package to the PYTHIA package. At the first step, the SingleTop generator simulates events at the parton level for the final particles. Then, the events are input to the PYTHIA MC generator using the CPYTH package. The PYTHIA package simulates parton emission (ISR/FSR), as well as hadronization and multiple interaction effects. Finally, the events might be developed to the simulation of the response from an actual detector. In such a setting, the MC generator preserves the correct spin structure of an event and, therefore, all spin correlations in decay events are taken into account. The samples of events of all necessary subprocesses were prepared for further investigation. These samples correspond to the first version of the SingleTop MC generator. All event files are available from the databases with the event samples of the CMS [25] and D0 [26] Collaborations.

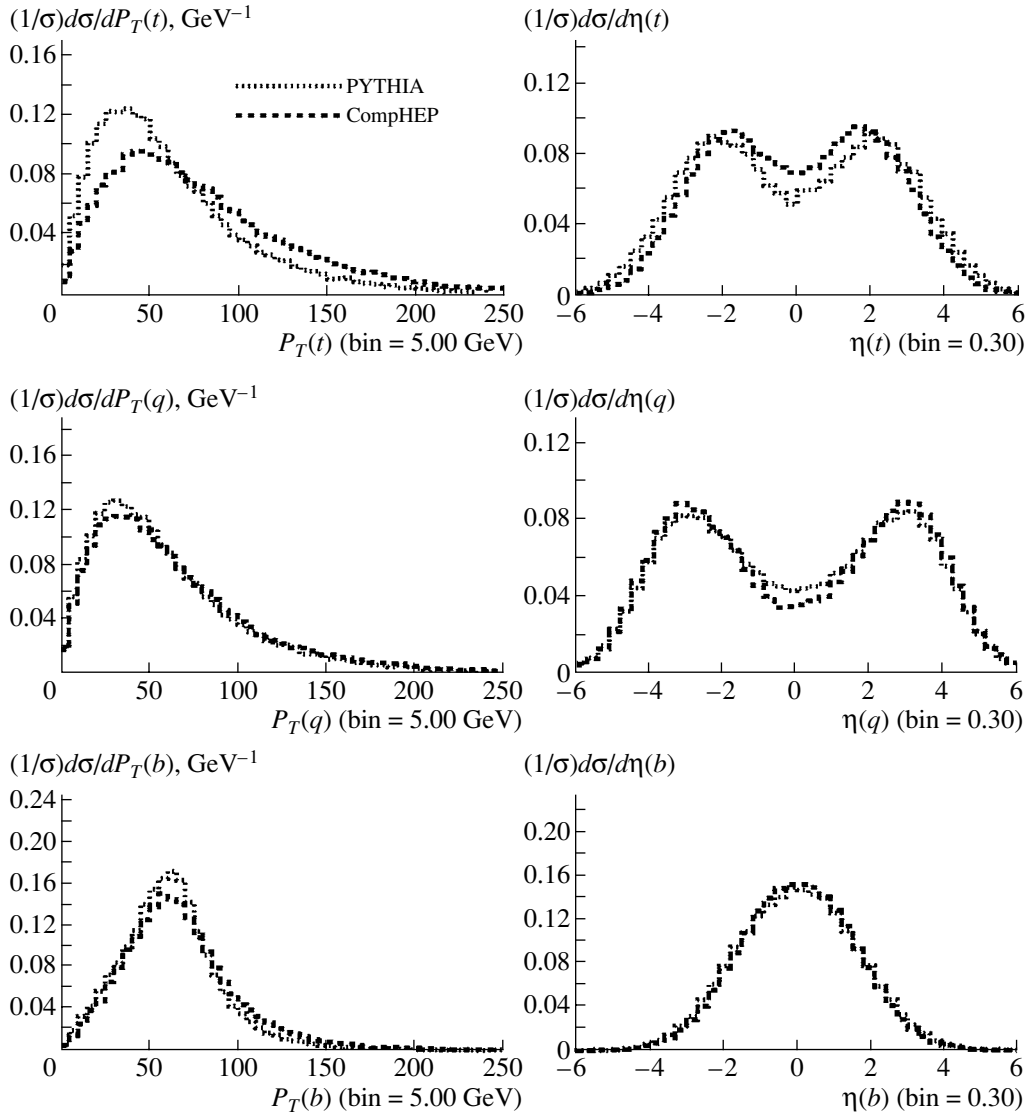## 3. METHOD OF EVENT SIMULATION IN THE EFFECTIVE NLO APPROXIMATION

The cross sections for the $pp \to tqb$ process (Table 3) are obtained in the LO approximation including the total set of the Feynman diagrams with the top quark appearing together with the additional b quark and the light quark in the final state (the $2 \to 3$ process[1]). However, the calculation of the $2 \to 3$ process in the tree approximation does not include large

logarithmic QCD corrections that are associated with the $g \to b\bar{b}$ graph and appear for low transverse momenta of the b quark. We can sum the corrections in the standard way and include them in the parton distributions of b quarks in the proton. In this case, the LO approximation for the t-channel process is the $2 \to 2$ reaction with the b quark in the initial state (the diagram in Fig. 1a and the cross sections in Table 4). Nevertheless, the b quark should anyway appear in the final state, because b quarks can appear in the proton only in pairs from an off-shell gluon ($g^* \to b\bar{b}$). The final b quark in the $2 \to 2$ process can be simulated by using the ISR mechanism in an MC generator such as the PYTHIA generator. An additional b quark will appear in one of the shower cascades, when we use the kernel of the $g^* \to b\bar{b}$ process.[2] One of two b quarks serves as the initial parton in the hard reaction, whereas the other quark appears in the final state. Below, we will show that the combination of the events for the $2 \to 2$ and $2 \to 3$ processes effectively generates NLO events.

The calculation of the $2 \to 3$ process in the tree approximation does not involve large logarithmic corrections associated with the $g^* \to b\bar{b}$ process, but reproduces the correct P_T behavior of the b quark in the hard region. On the other hand, introducing the parton distribution for the b quarks and using the ISR mechanism to simulate the final b quark, one can generate events with the correctly simulated soft b quark, but the contribution from the hard $P_T(b)$ region is significantly underestimated. Thus, we should

---

[1] We notice that all events for the MC generator are prepared with the decayed top quark; therefore, the process name $2 \to 3$ is rather conditional in this case. At the parton level, the process is $2 \to 5$, where three particles are the decay products of the top quark and two particles are two additional quarks.

[2] The b-quark behavior for soft transverse momenta was discussed in [27, 28].

Fig. 4. Particle distributions in the transverse momentum P_T and pseudorapidity η for the $pp \to tq + b_{ISR}$ (simulated using the PYTHIA package) and $pp \to tq + b_{LO}$ (calculated using the CompHEP package) processes at the LHC collider without kinematic cutoff. The distributions are normalized to unity.

use different approximations in different $P_T(b)$ regions. Unfortunately, it is impossible to combine the samples of the $2 \to 2$ and $2 \to 3$ processes in a naive, straightforward way, because the contribution from a certain part of the phase space would be included twice. The double counting problem can be solved by separating the regions where individual calculation methods are used with respect to a certain typical kinematic parameter.

Figures 4–7 show the distributions normalized to unity that are obtained by two different calculation methods for the Tevatron and LHC colliders. The P_T and pseudorapidity distributions of the top quark coincide with the respective distributions of the light quark for both the LHC (Fig. 4) and the Tevatron

(Fig. 6). However, the distributions for the additional b quark (produced not owing to the decay of the top quark) are significantly different (Figs. 5 and 7). The distribution in pseudorapidity $\eta(b)$ has peaks at larger values of $\eta(b)$ as compared to the distributions obtained with the tree matrix element $2 \to 3$. In the latter case, b quarks are distributed in the central region, while the $P_T(b)$ spectrum simulated by the ISR mechanism in the PYTHIA MC generator is softer in agreement with our expectation. If we apply the kinematic cutoff $P_T(b) > 20$ GeV, the cross section for the $pp \to tq + b_{LO}$ (116 pb) process generated with the complete matrix element would be several times larger than the cross section for the $2 \to tq + b_{ISR}$ process (25.4 pb).

The main contribution of large logarithmic corrections appears in the soft $P_T(b)$ region. Therefore, it is reasonable to choose the transverse momentum of the additional b quark as the kinematic parameter for separating the soft and hard regions. Then, in order to generate NLO events, we apply the following procedure. In the hard $P_T(b)$ region above a certain threshold P_T^0, we take events for the $2 \to 3$ process with the cross section calculated using the CompHEP package. In the soft region, we take the events for the $2 \to 2$ process with the cross section multiplied by a certain K factor in order to include loop corrections, which weakly change the event kinematics. The K factor is calculated from the normalization condition of the cross section for the obtained event sample to the NLO total cross section for the t-channel process:

$$\sigma_{\text{NLO}} = K\sigma_{\text{PYTHIA}}(2 \to 2)|_{P_T(b)<P_T^0}$$
$$+ \sigma_{\text{CompHEP}}(2 \to 3)|_{P_T(b)>P_T^0}.$$

It is seen that the coefficient K is a function of the matching parameter P_T^0. For example, in the case of the LHC collider, we obtain

$$\sigma_{\text{CompHEP}}(2 \to 3)|_{P_T(b)>20\,\text{GeV}} \approx 108.7 \text{ pb},$$
$$\sigma_{\text{CompHEP}}(2 \to 3)|_{P_T(b)>10\,\text{GeV}} \approx 125.7 \text{ pb}$$

and $K = 0.89$ for $P_T^0 = 20$ GeV and $K = 0.77$ for $P_T^0 = 10$ GeV. For the Tevatron collider, we obtain

$$\sigma_{\text{CompHEP}}(2 \to 3)|_{P_T^b>20\,\text{GeV}} \approx 0.46 \text{ pb},$$
$$\sigma_{\text{CompHEP}}(2 \to 3)|_{P_T^b>10\,\text{GeV}} \approx 0.72 \text{ pb}$$

and $K = 1.32$ for $P_T^0 = 20$ GeV and $K = 1.21$ for $P_T^0 = 10$ GeV.

The natural criterion for the correct determination of the matching parameter $P_T^0(b)$ is the smoothness of the P_T distribution for the additional b quark in the whole kinematic region. Figures 8 and 9 show the matching results at the value $P_T^0(b) = 20$ GeV. We can observe a prominent convexity in the matching region. After certain investigation, we found that the $P_T(b)$ distribution becomes smooth at a matching parameter of $P_T^0(b) = 10$ GeV. Figures 10 and 11 show the corresponding distributions. Therefore, the boundary between the soft and hard regions is $P_T^0(b) = 10$ GeV and thereby the event generation procedure is completed in the whole phase space. We refer to this algorithm as the effective NLO approximation.

4. COMPARISON OF THE EFFECTIVE AND EXACT NLO APPROXIMATIONS

Sullivan[9] demonstrated that the NLO results for the s-channel process completely coincide with the
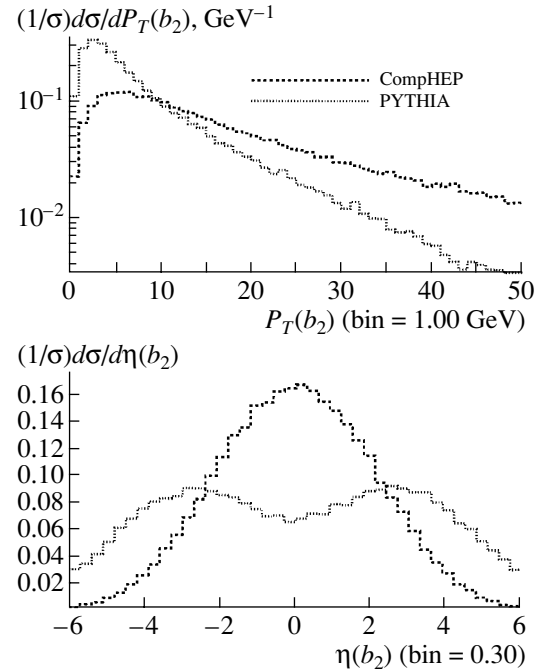
Fig. 5. Distributions of the additional final b quark in the transverse momentum P_T and pseudorapidity η in the t-channel process for the LHC collider without kinematic cutoff. The CompHEP and PYTHIA curves refer to the $pp \to tq + b_{\text{LO}}$ and $pp \to tq + b_{\text{ISR}}$ processes, respectively. The distributions are normalized to unity.

LO calculations with the accuracy to the K factor. Therefore, the LO and NLO distributions coincide with each other.

The event simulation method described in the preliminary section enables one to simulate events with the single top-quark production in the t-channel process including the NLO corrections. In order to clearly demonstrate the validity of such an approach, we compared the most indicative distributions obtained on the basis of the generated event sample with the exact NLO distributions. We performed the comparison with the results of two NLO independent calculations. The ZTOP [9] and MCFM [10] code packages can calculate the kinematic distributions including the NLO corrections. In ZTOP, the top quark is simulated disregarding its decay, while the MCFM package includes the NLO corrections also in the decay of the top quark.[3] For this reason, we compared the distributions of the final quarks in the transverse momentum and in the pseudorapidity for the ZTOP and SingleTop software modules. The distributions shown in Fig. 12 are in good agreement

---

[3] It is worth noting that the SingleTop generator simulates events with the parton showers for the final quarks; in this way, the SingleTop includes the most part of the NLO corrections to the decay of the top quark.
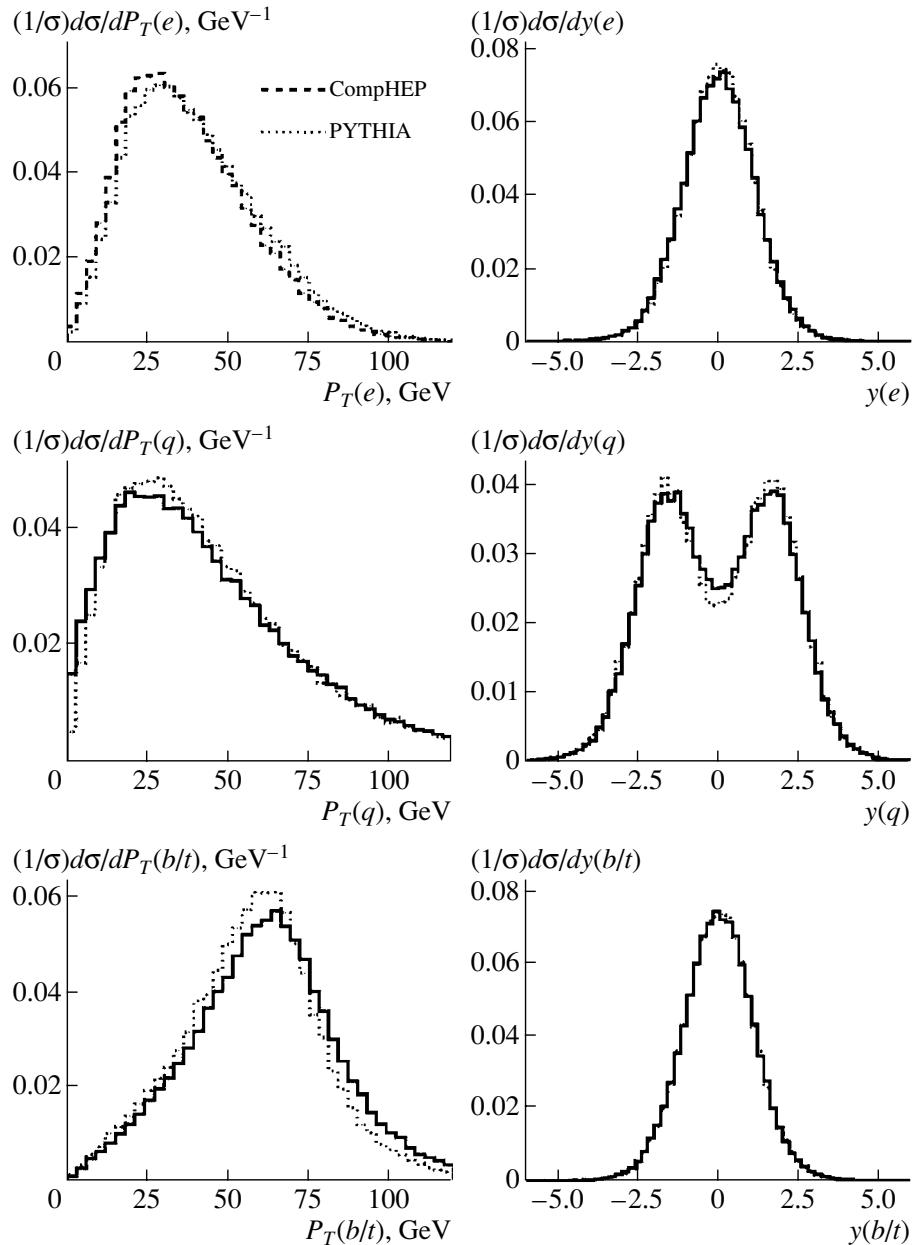
Fig. 6. The same as in Fig. 4, but for the Tevatron collider.

with each another. The SingleTop and MCFM calculations of the distributions of the leptons from the decay of the top quark in the transverse momentum and pseudorapidity are shown in Fig. 13. These distributions also almost coincide with each other.

The comparison demonstrates excellent agreement of the distributions obtained by the SingleTop MC generator and the ZTOP and MCFM code packages for all objects in the final state of the t-channel process, which gives additional support for the proposed approach to the event simulation by the method of the effective NLO approximation.

5. SPIN CORRELATIONS IN THE SINGLE TOP-QUARK PRODUCTION PROCESSES

The top quark is produced in the s-channel process in the Wtb vertex, which has the $(V - A)$ structure. As a result, the top quark is highly polarized. It is easy to show that the spin projection axis corresponding to the maximum polarization is the momentum direction of the $\bar{d}$ quark from the initial state in the rest frame of the top quark [18]. Owing to the correspondence between the decay and production diagrams of the top quark (the diagrams are topologically equivalent), the best probe for the top quark spin is
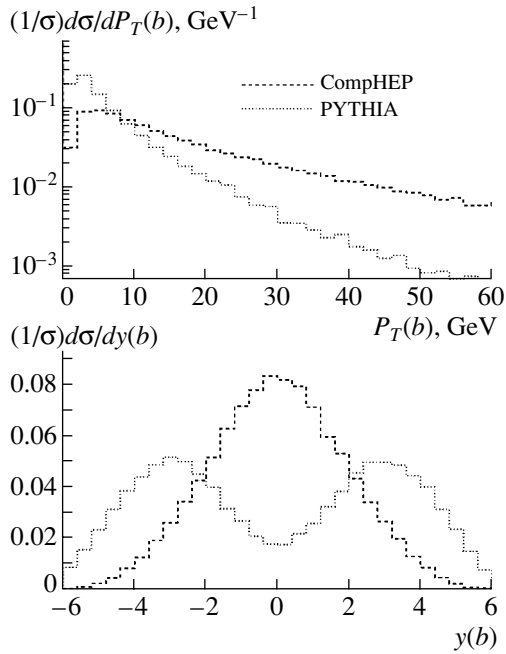
Fig. 7. The same as in Fig. 5, but for the Tevatron collider.

Fig. 8. Distributions for the b quark after the combination of events for the $pp \to tq + b_{\mathrm{ISR}}$ (calculated using the PYTHIA generator) and $pp \to tq + b_{\mathrm{LO}}$ (calculated using the CompHEP package) processes at the LHC collider with the matching parameter $P_T^0(b) = 20$ GeV.

its decay-product lepton [19]. Thus, the best variable to observe spin correlations in the s-channel process is the cosine of the angle between the momenta of the initial $\bar{d}$ quark and the lepton in the rest frame of the top quark. Spin correlations can be numerically characterized by the coefficient R_{spin} of $\cos \theta^*_{e^+,\bar{d}}$ in the normalized distribution

$$\frac{1}{\sigma}\frac{d\sigma}{d\cos\theta^*_{e^+,\bar{d}}} = \frac{1 + R_{\mathrm{spin}}(\bar{s})\cos\theta^*_{e^+,\bar{d}}}{2}.$$

Then, $R_{\mathrm{spin}}(\bar{p}_d) = 1$ (or 100%) for the s-channel process. Since the NLO approximation is manifested only in the K factor in this process, we do not expect any significant reduction of R_{spin} owing to the inclusion of NLO corrections.

The diagram of the t-channel process in the LO approximation is also topologically equivalent to the decay diagrams of the s-channel process. Thus, the top quark is polarized, and the axis of the maximum polarization is the momentum of the final light quark in the rest frame of the top quark. The dotted histogram in Fig. 14 corresponds to LO events. The first-order polynomial fit to the distribution gives $R_{\mathrm{spin}}(\bar{p}_d)_{\mathrm{LO}} = 0.98 \pm 0.02$, which indicates the maximum polarization of the top quark in the LO approximation. In the NLO approximation, a significant contribution comes from the real correction with the additional b quark. In this process, the top quark can be produced in the QCD vector interaction vertex with the gluon, which reduces the polarization of the top quark. However, this reduction is not strong
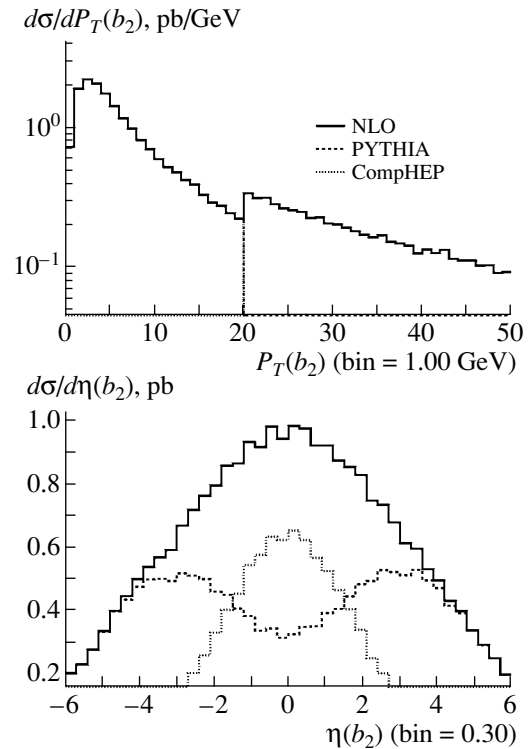

Fig. 9. The same as in Fig. 8, but for the Tevatron collider.

$dN_{\text{event}}/dP_T(t)$, GeV^{-1}

$dN_{\text{event}}/d\eta(t)$

$dN_{\text{event}}/dP_T(b)$, GeV^{-1}

$dN_{\text{event}}/d\eta(b)$

Fig. 10. Distributions after the combination of events for the $pp \to tq + b_{\text{ISR}}$ (simulated by the PYTHIA generator) and $pp \to tq + b_{\text{LO}}$ (calculated using the CompHEP package) processes at the LHC collider with the matching parameter $P_T^0(b) = 10$ GeV.
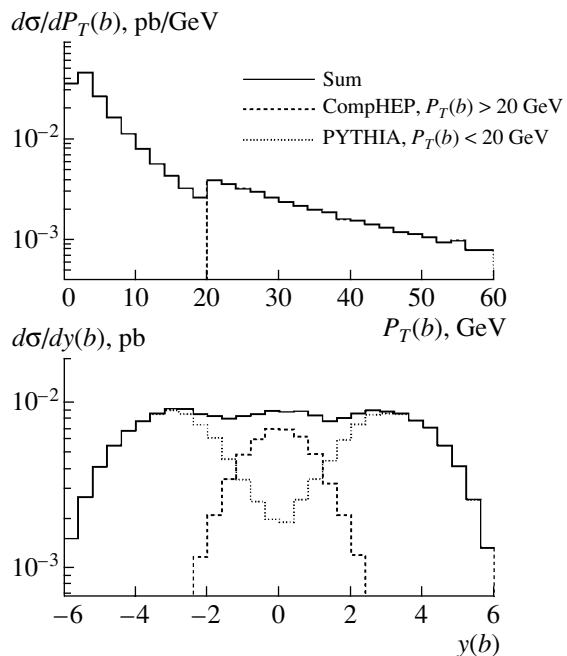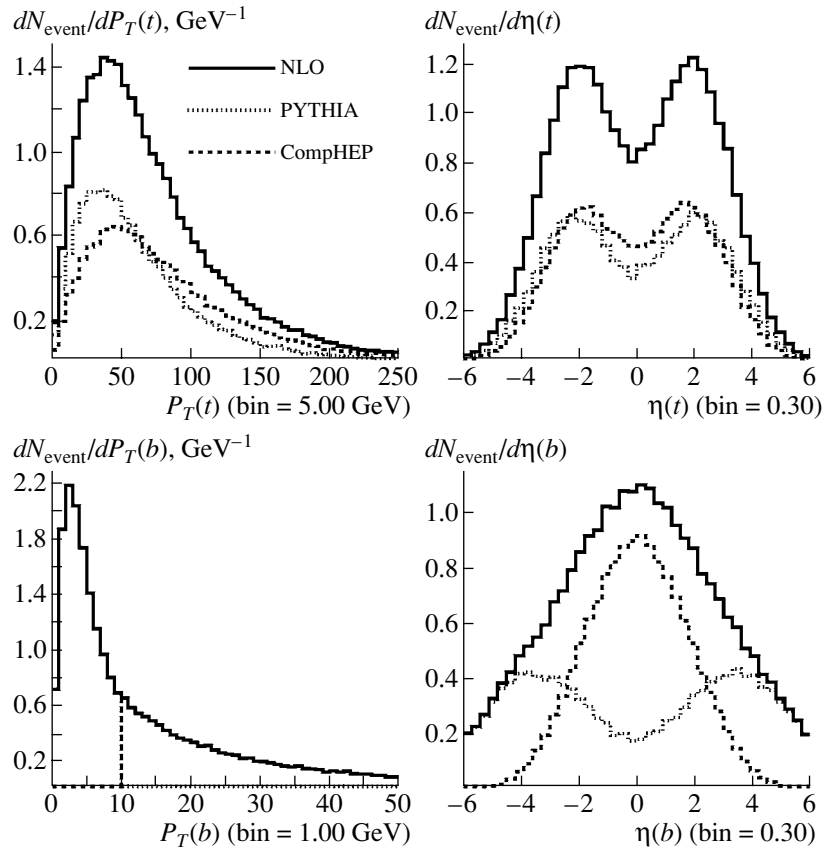
because the main contribution to the $pp \to tqb$ process comes from the diagram with the Wtb production vertex of the top quark. The solid histogram in Fig. 14 shows the distribution of the NLO events in $\cos\theta^*_{l^+,d}$. The straight-line fit of the distribution gives $R_{\text{spin}}(\bar{p}_d)_{\text{NLO}} = 0.89 \pm 0.02$, which indicates the insignificant reduction of the polarization value.

The tW process requires special consideration. The leading order Feynman diagrams for this process include two diagrams; in one of them, the top quark is produced in the QCD interaction vertex with the gluon, and its contribution to the total cross section is comparable to the electroweak-interaction contribution. In [19], it was shown how to increase the polarization of the top quark from the initial 24 to 80−90% by means of cutoffs with respect to certain kinematic variables.

It is worth noting that the measurement of the top-quark polarization is a difficult task in all processes. First, it is necessary to reconstruct the rest frame of the top quark with maximum possible precision, because measurements should be performed in this reference frame. Second, the kinematic cutoffs that are required to separate trigger events might be correlated with the spin variables, which complicates the measurement of the R_{spin} value in a real experiment. However, the study of spin effects in single top-quark production processes is an important problem, because it provides the possibility of testing the SM in the sector of the third-generation fermions and searching for the deviations from the SM.

6. CONCLUSIONS

We developed a method for simulating electroweak top-quark production events. This method allows the effective inclusion of the NLO corrections at the event generation level and the solution of such problems as the appearance of negative-weight events and double counting of certain Feynman diagrams. On the basis of this method, we created the first version of the SingleTop Monte Carlo generator. The created package was used to generate various samples of single top-quark production events in the t- and s-channel processes for the Tevatron and the LHC colliders. The generated events are used by the D0 and the CMS Collaborations in the experimental analyses and are
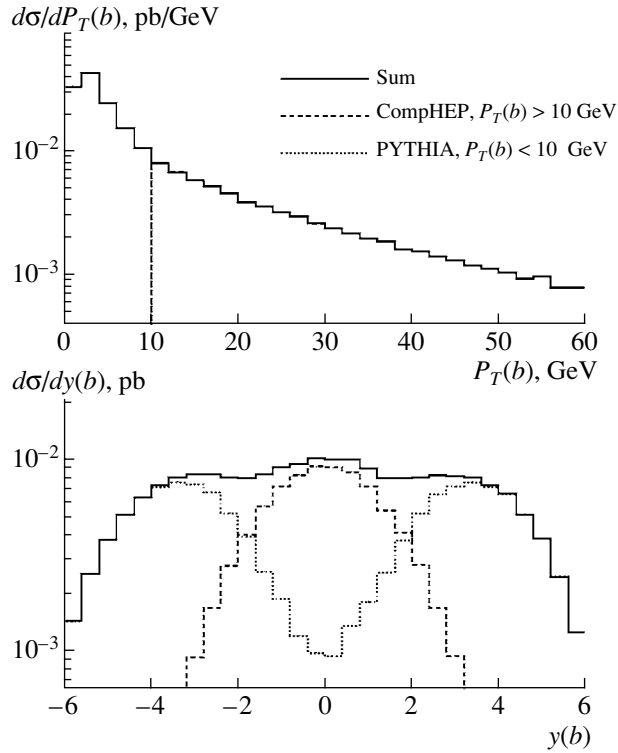
$d\sigma/dP_T(b)$, pb/GeV

Sum

CompHEP, $P_T(b) > 10$ GeV

PYTHIA, $P_T(b) < 10$ GeV

$P_T(b)$, GeV

$d\sigma/dy(b)$, pb

$y(b)$

Fig. 11. The same as in Fig. 10, but for the Tevatron collider.

$(1/\sigma)d\sigma/dP_T(\text{light quark})$, GeV^{-1}

CompHEP

ZTOP   ++++

$P_T(\text{light quark})$ (bin = 4 GeV)

$(1/\sigma)d\sigma/dP_T(t)$, GeV^{-1}

$P_T(t)$ (bin = 4 GeV)

$(1/\sigma)d\sigma/dP_T(b)$, GeV^{-1}

$P_T(b)$ (bin = 1 GeV)
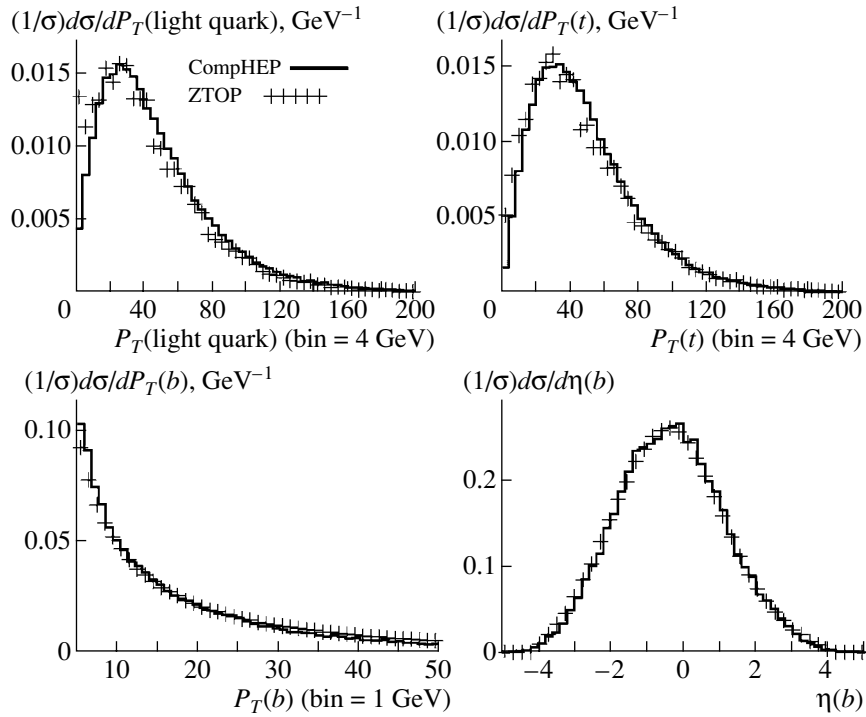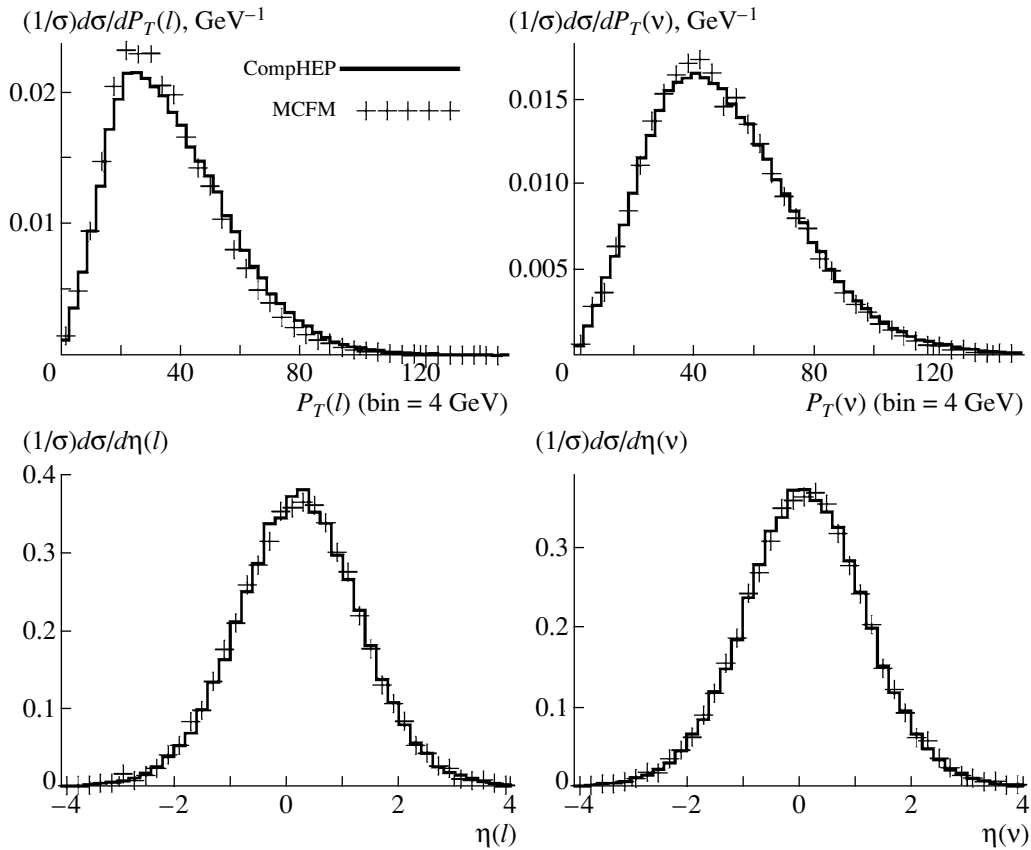
$(1/\sigma)d\sigma/d\eta(b)$

$\eta(b)$

Fig. 12. Distributions of the final quarks in the transverse momentum and pseudorapidity in the effective NLO approximation (simulated by the SingleTop generator) and in the exact NLO approximation (obtained by the ZTOP code) for the Tevatron collider.

Fig. 13. Distributions in the transverse momentum and pseudorapidity for the lepton and neutrino from the decay of the top quark in the effective NLO approximation (simulated by the SingleTop generator) and in the exact NLO approximation (calculated by the MCFM code) for the Tevatron collider.
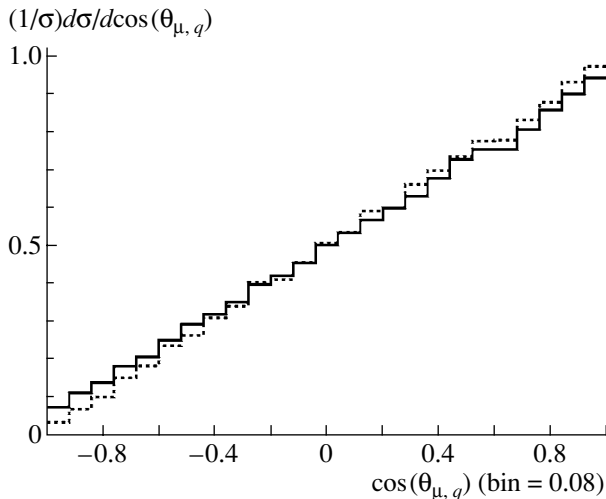
Fig. 14. Distribution in the cosine of the angle between the momenta of the light quark and lepton from the decay of the top quark in its rest frame. As shown in [19], this variable is the best to observe spin correlations in the t-channel process. The solid and dotted histograms correspond to the NLO and LO events, respectively.

available from the event sample databases FNAL MCDB [26] and CMS MCDB [25], respectively.

We found that the value $P_T^0(b) = 10$ GeV is a boundary between the hard and soft regions of the transverse momentum P_T of the additional final b quark in the t-channel process. The hard and soft regions require different methods for calculating the cross sections and event simulation. Events with $P_T^0(b) > 10$ GeV are generated by the code part of the SingleTop MC generator that includes the complete set of tree diagrams for the $pp(p\bar{p}) \rightarrow tjb$ process. Events with $P_T^0(b) < 10$ GeV are generated by the code part for the $pp(p\bar{p}) \rightarrow tj$ process, where the additional b quark appears in the parton shower in the initial state. The PYTHIA MC generator is used for shower simulation. The hard and soft regions form the complete phase space for the $pp(p\bar{p}) \rightarrow tjb$ process, and the cross section in the soft region is normalized so that the total cross section is equal to $\sigma_{\rm NLO}$ for the t-channel process. The procedure of matching the event samples is called the method of event simulation in the effective NLO approximation.

The SingleTop MC generator based on the

CompHEP package for symbolic and numerical calculations includes NLO corrections in the production and decay of the top quark, spin correlations for the top quark, and finite widths of the top quark and W boson. It can simulate the t- and $\bar{t}$-quark production processes separately both in the SM and with the inclusion of the FCNC vertices and anomalous contributions to the Wtb vertex [20] (magnetic moments of the particles and $(V + A)$ structure). The SingleTop MC generator involves all details of the current understanding of the single top-quark production processes and is a powerful tool for the phenomenological analysis of processes involving the top quark.

ACKNOWLEDGMENTS

REFERENCES

1. F. Abe et al. (CDF Collab.), Phys. Rev. Lett. **74**, 2626 (1995) [hep-ex/9503002]; S. Abachi et al. (D0 Collab.), Phys. Rev. Lett. **74**, 2632 (1995) [hep-ex/9503003].

2. P. A. Movilla Fernandez (CDF Collab.), Nucl. Phys. B (Proc. Suppl.) **142**, 408 (2005) [hep-ex/0409001]; V. M. Abazov et al. (D0 Collab.), Nature **429**, 638 (2004) [hep-ex/0406031].

3. S. S. D. Willenbrock and D. A. Dicus, Phys. Rev. D **34**, 155 (1986); C. P. Yuan, Phys. Rev. D **41**, 42 (1990); G. V. Dzhikia and S. R. Slabospitsky, Sov. J. Nucl. Phys. **55**, 1387 (1992); Phys. Lett. B **295**, 136 (1992); R. K. Ellis and S. J. Parke, Phys. Rev. D **46**, 3785 (1992); G. Bordes and B. van Eijk, Z. Phys. C **57**, 81 (1993); Nucl. Phys. B **435**, 23 (1995); S. Cortese and R. Petronzio, Phys. Lett. B **253**, 494 (1991); D. O. Carlson, E. Malkawi, and C. P. Yuan, Phys. Lett. B **337**, 145 (1994) [hep-ph/9405277]; T. Stelzer and S. Willenbrock, Phys. Lett. B **357**, 125 (1995) [hep-ph/9505433]; R. Pittau, Phys. Lett. B **386**, 397 (1996) [hep-ph/9603265]; D. Atwood, S. Bar-Shalom, G. Eilam, and A. Soni, Phys. Rev. D **54**, 5412 (1996) [hep-ph/9605345]; C. S. Li, R. J. Oakes, and J. M. Yang, Phys. Rev. D **55**, 1672, 5780 (1997) [hep-ph/9608460, hep-ph/9611455]; T. Stelzer, Z. Sullivan, and S. Willenbrock, Phys. Rev. D **56**, 5919 (1997) [hep-ph/9705398]; S. Bar-Shalom, G. Eilam, A. Soni, and J. Wudka, Phys. Rev. D **57**, 2957 (1998) [hep-ph/9708358]; T. Tait and C. P. Yuan, hep-ph/9710372.

4. B. W. Harris et al., Phys. Rev. D **66**, 054024 (2002) [hep-ph/0207055].

5. A. P. Heinson, A. S. Belyaev, and E. E. Boos, Phys. Rev. D **56**, 3114 (1997) [hep-ph/9612424].

6. A. S. Belyaev, E. E. Boos, and L. V. Dudko, Phys. Rev. D **59**, 075001 (1999) [hep-ph/9806332].

7. M. C. Smith and S. Willenbrock, Phys. Rev. D **54**, 6696 (1996) [hep-ph/9604223].

8. T. Stelzer, Z. Sullivan, and S. Willenbrock, Phys. Rev. D **58**, 094021 (1998) [hep-ph/9807340].

9. Z. Sullivan, Phys. Rev. D **70**, 114012 (2004) [hep-ph/0408049].

10. J. Campbell, R. K. Ellis, and F. Tramontano, Phys. Rev. D **70**, 094012 (2004) [hep-ph/0408158].

11. Q. H. Cao, R. Schwienhorst, and C. P. Yuan, Phys. Rev. D **71**, 054023 (2005) [hep-ph/0409040].

12. T. Stelzer, Z. Sullivan, and S. Willenbrock, Phys. Rev. D **56**, 5919 (1997) [hep-ph/9705398].

13. D. O. Carlson and C. P. Yuan, Phys. Lett. B **306**, 386 (1993).

14. S. R. Slabospitsky and L. Sonnenschein, Comput. Phys. Commun. **148**, 87 (2002) [hep-ph/0201292].

15. F. Maltoni and T. Stelzer, JHEP **0302**, 027 (2003) [hep-ph/0208156].

16. E. Boos et al., Nucl. Instrum. Methods Phys. Res. A **534**, 250 (2004) [hep-ph/0403113].

17. T. Sjostrand et al., Comput. Phys. Commun. **135**, 238 (2001) [hep-ph/0010017].

18. G. Mahlon and S. J. Parke, Phys. Rev. D **55**, 7249 (1997) [hep-ph/9611367]; Phys. Lett. B **476**, 323 (2000) [hep-ph/9912458].

19. E. E. Boos and A. V. Sherstnev, Phys. Lett. B **534**, 97 (2002) [hep-ph/0201271].

20. E. Boos, L. Dudko, and T. Ohl, Eur. Phys. J. C **11**, 473 (1999) [hep-ph/9903215].

21. E. Boos, L. Dudko, and V. Savrin, CMS Note 2000/065.

22. A. Belyaev and E. Boos, Phys. Rev. D **63**, 034012 (2001) [hep-ph/0003260]; T. M. P. Tait, Phys. Rev. D **61**, 034001 (2000) [hep-ph/9909352].

23. J. Pumplin et al., JHEP **0207**, 012 (2002) [hep-ph/0201195].

24. V. Ilyin et al., hep-ph/0101232.

25. http://cmsdoc.cern.ch/cms/generators/mcdb/

26. http://www-d0.fnal.gov/~dudko/mcdb/

27. J. Campbell et al., hep-ph/0405302.

28. E. Boos and T. Plehn, Phys. Rev. D **69**, 094005 (2004) [hep-ph/0304034].

Translated by M. Kobrinsky